Machine Vision and Applications (2011) 22:819–835
DOI 10.1007/s00138-011-0327-y

ORIGINAL PAPER

Automatic LightBeam Controller for driver assistance

P. F. Alcantarilla · L. M. Bergasa · P. Jiménez · I. Parra · D. F. Llorca · M. A. Sotelo · S. S. Mayoral

Received: 25 May 2009 / Revised: 26 November 2010 / Accepted: 10 February 2011 / Published online: 27 March 2011
© Springer-Verlag 2011

Abstract In this article, we present an effective system for detecting vehicles in front of a camera-assisted vehicle (preceding vehicles traveling in the same direction and oncoming vehicles traveling in the opposite direction) during night-time driving conditions in order to automatically change vehicle head lights between low beams and high beams avoiding glares for the drivers. Accordingly, high beams output will be selected when no other traffic is present and will turn low beams on when other vehicles are detected. In addition, low beams output will be selected when the vehicle is in a well lit or urban area. LightBeam Controller is used to assist drivers in controlling vehicle's beams increasing its correct use, since normally drivers do not switch between high beams and low beams or vice versa when needed. Our system uses a B&W forward looking micro-camera mounted in the windshield area of a C4-Picasso prototype car. Image processing techniques are applied to analyse light sources and to detect vehicles in the images. Furthermore, the system is able to classify between vehicle lights and road signs reflections or nuisance artifacts by means of support vector machines. The algorithm is efficient and able to run in real time. The system has been tested with different video sequences (more than 7 h of video sequences) under real night driving conditions in different roads of Spain. Experimental results, a comparison with other representative state of the art methods and conclusions about the system performance are presented.

Keywords Computer vision · Driver-assistance systems · Head-lights detection · Tail-lights detection · Support vector machines

P. F. Alcantarilla · L. M. Bergasa (✉) · P. Jiménez · I. Parra
Department of Electronics, University of Alcalá,
Alcalá de Henares, Madrid, Spain
e-mail: bergasa@depeca.uah.es

P. F. Alcantarilla
e-mail: pablo.alcantarilla@depeca.uah.es

P. Jiménez
e-mail: pjimenez@depeca.uah.es

I. Parra
e-mail: parra@depeca.uah.es

D. F. Llorca · M. A. Sotelo
Department of Automation, University of Alcalá,
Alcalá de Henares, Madrid, Spain
e-mail: llorca@aut.uah.es

M. A. Sotelo
e-mail: sotelo@aut.uah.es

S. S. Mayoral
FICO MIRRORS, SA, Research Department,
Mollet del Vallés, Barcelona, Spain
e-mail: silvia.sanchezmayoral@ficosa.com

1 Introduction

Modern automotive vehicles include a variety of different lamps to provide illumination under different operating conditions. Headlamps are typically controlled to alternately generate low beams and high beams. Low beams provide less illumination and are used at night to illuminate the forward path when other vehicles are present. High beams provide significantly more light and are used to illuminate the vehicle's forward path when other vehicles are not present. Daylight running lights have also begun to experience widespread acceptance.

There are various countries with regulations to control the amount of glare experienced by drivers due to preceding vehicles (other vehicles traveling in the same direction) and oncoming vehicles (vehicles traveling in the opposite

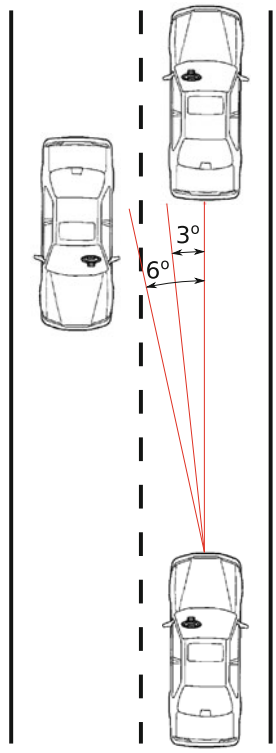

Fig. 1 Scheme of the dimming vehicle high beam headlamps problem

direction). These laws obligate vehicle manufacturers to build vehicles that comply with these regulations. For example, the Department of Transportation (DOT) in USA [1] regulates the light emissions of vehicle high beam headlamps. In accordance with the DOT regulation limits, vehicle high beam headlamp emissions provide an intensity of 40,000 cd at 0°, 10,000 cd at 3°, 3,250 cd at 6°, 1,500 cd at 9° and 750 cd at 12°. A scheme for understanding this problem is illustrated in Fig. 1. In order to avoid an illuminance of 0.1 foot-candles (fc) incident on another vehicle at these angles, the vehicle high beams headlamps should be dimmed within 700 feet (213 m) of another vehicle at 0°, within 350 feet (107 m) of another vehicle at a horizontal position of 3° and 200 feet (61 m) of another vehicle at a horizontal position of 6°. In order to prevent other vehicles drivers from being subjected to excessive glare levels an automatic control of the vehicle headlamps can be done. For a preceding vehicle, the distance by which the controlled vehicle's headlamps must be dimmed, can be less than for an oncoming vehicle since glare form behind is usually less disruptive than oncoming glare. In the last few years many researchers have studied the effects of oncoming headlight glare [2]. An automatic headlamp dimmer system must sense both the head lights of the oncoming vehicles as well as the tail lights of preceding vehicles. Then, it has to distinguish between nuisance light sources, such as reflections of road signs or road reflectors, streetlights, etc., from light sources that require headlight control to avoid an undesirable performance.

Several automatic headlamp dimmer control systems have been proposed in the literature by automobile manufacturers but, from our knowledge, at the moment none of them are commercialized. However, there are only few references in specialized scientific journals and symposiums. Currently the two more relevant systems developed by automobile manufacturers are:

- SmartBeam, a vehicle lamp control developed by Gentex Corporation. It is a system and method for automatically controlling vehicle headlamps including an image sensor and a controller to generate headlamp control signals. The result is an intelligent, high-beam headlamp control system that greatly improves night-time driving safety. SmartBeam optimizes the use of a vehicle's headlamp system in order to provide the maximum amount of light possible for any driving scenario [3].
- Adaptive headlight control (AHC) developed by Mobileye. The system is intended to support the driver in using the high beam to the fullest extent possible, without inconveniencing oncoming or preceding traffic. To perform AHC Mobileye uses an image grabber and detailed analysis of light sources appearing in the image. The AHC Mobileye's system turns the high beams off in the following cases:

  1. Preceding traffic (tail lights): where tail lights are recognized in front of the host vehicle up to a distance of 400 m.
  2. Oncoming traffic (head lights): whenever there is an oncoming vehicle up to a distance of 800 m.
  3. Lit/Urban areas: whenever the host vehicle enters a well lit (or an urban) area.

  According to its Web page Mobileye's AHC will be in serial development in the next future with for a major European platform [4].

Normally drivers do not switch properly between low and high beams or vice versa. Instead, drivers keep low beams on in order to avoid frequent switching and often forget to turn high beams off or switch beams too late. In fact, this can contribute to accidents due to excessive glares. Moreover, driving under or with low beams reduces the drivers visibility range which reduces the ability of response to possible traffic events ahead such as pedestrians.

Under night-time driving conditions the more confident visual information for detecting vehicles are their head lights and tail lights. Some researchers have been working on the development of systems for night-time vehicle detection and they are based mainly in the detection of head lights and tail lights. In [5] head lights and tail lights are extracted by means of an automatic multilevel thresholding using a colour camera. Then bright objects are processed by a rule-based procedure, to identify the vehicles by locating and analyzing their vehicle light patterns, and estimate their distances

to the camera-assisted car. However, the results about distance detection (they only show results up to 23 m) are very poor for a real application. Generally it is recommended to dim high beams for a preceding vehicle at least a distance of 100 m and for an oncoming vehicle at a distance of 200 m. In addition, their proposed method for dealing with nuisance artifacts such as road signs is not robust enough. They simply discard the first one-third of the vertical y-axis, which in fact is a dangerous assumption which can reduce drastically the distance detection range. For far detection distances, a robust headlamp controller must deal and classify correctly between nuisance artifacts, road sign's reflections, head lights and tail lights. In [6] a similar approach for night-time vehicle detection is proposed. In this case only tail lights are detected and only results up to 30 m are shown. Then, classification method used to deal with nuisance artifacts are only based in aspect ratio constraints. In conclusion, this approach presents the same limitation, even more, than the previous one. In [7] another approach for an intelligent headlight control is proposed. They use a novel image sensor where 75% of the pixels are monochrome and 25% are red for improving the detection of vehicular lamps at far distances. For dealing with nuisance artifacts and reflections, they propose using Real-AdaBoost machine learning [8] with a large number of vehicular features both in B&W and colour. Although, their method and the use of their novel sensor seems to be promising, they just only have a qualitative (non-quantitative) impression of system performance.

In [9] the bases of our LightBeam Controller are explained and some preliminar results presented. In this article, more details about the system and results are analysed. Our work proposes an effective automatic control of the vehicle headlamps based on the detection of head lights and tail lights under night-time road conditions. LightBeam Controller uses a B&W camera, since for an industry mass production it is cheaper using B&W micro-cameras than colour cameras. Besides, the sensitivity of B&W cameras is higher than for colour ones. This is a very important topic for a visual system that must work under night-time conditions. Higher B&W sensitivity makes possible the detection of bright lamps at far distances. The main stages of the algorithm are explained in Sect. 2. Experimental results can be found in Sect. 3. Conclusions and future works are presented in Sect. 4.

2 Algorithm

Our method comprises the following steps: the input images are obtained from the vision system using a B&W camera (CMOS image sensor) which is mounted behind the windscreen inside the camera-assisted vehicle.

In order to choose the optimal lens for this application, we did a geometrical study using a pin-hole model. The camera must see an oncoming vehicle as far as possible and it must hold this in its field of view until about 10 m away from the assisted car and with the minimum distortion. Then, it must be considered that a vehicle that is overtaking the assisted car must be detected before that its own head lights glare the driver of the other vehicle. From this study we concluded that the optimal lenses were between 4.3 and 6 mm of focal length. Figure 2 depicts the scenario for theses lenses.

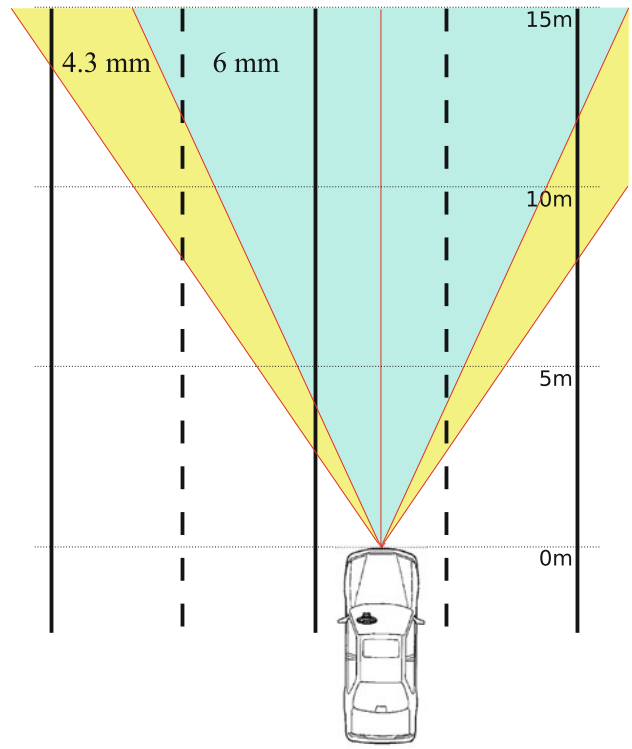

Fig. 2 Geometrical study for optical lenses

We performed some experimental tests using these two lenses for obtaining the best option in an experimental way. The results of these experiments concluded that for the lens of 6 mm bright objects appear in the image very close to the horizon line and the variation in vertical pixels from the frame where the vehicle appears in the image to the frame where it leaves this, is smaller than using the 4.3 mm lens. Then, the number of frames where the vehicle is in the field of view of the camera is lower for the 6 mm than for the 4.3 mm focal distance. On the other hand, for uneven roads vehicles can be seen with a 4.3 mm lens before than using a 6 mm one due to its higher field of view. Finally, when a vehicle is overtaking the assisted car, with a 4.3 mm lens the vehicle is detected before than with a 6 mm one, minimizing the glare of the driver. As conclusion, the optical lens was set to 4.3 mm, because its field of view is closer to the human one and with this lens, vehicle detection performance is higher. In addition, with our camera settings we can use the same camera configuration for other driver assistance applications

Fig. 3 Typical night-time road environment

addressable by a monocular B&W camera system, such as lane departure warning [10] or pedestrian detection [11].

As can be seen in Fig. 3, typical night-time road conditions are characterized by a dark background and bright objects corresponding to vehicular lamps and nuisance light sources (reflections of road signs or road reflectors, streetlights, etc.). In order to distinguish between vehicular lamps and nuisance artifacts, we propose to maximize the halo effect. In order to do that, we have to pay special attention to the camera settings as we will explain hereafter.

An overall overview of our algorithm is depicted in Fig. 4. Firstly, an adaptive thresholding must be applied to detect bright blobs in the image, which correspond to with vehicles' lights. Vehicular lamp usually correspond to bright objects in the image under night-time driving conditions. According to this, a good image processing starting point seems to be some form of thresholding. In [5] they perform an automatic multilevel thresholding for bright objects extraction under night-time driving conditions. They transform RGB images into grey-intensity images to reduce the computation time of the segmentation, and apply their multilevel segmentation algorithm based in the work by Otsu [12]. In [6] they detect tail lights by applying two colour threshold to search for white and red regions transforming RGB space to Hue, Saturation, Value (HSV) colour space since this colour space is more representative of the way humans observe colour. Using colour information is an effective way to reduce the effect of nuisance artifacts and remove non-vehicle light sources, and also it benefits the detection of tail lights. However, for RGB cameras the sensor sensitivity for bright objects is smaller than for B&W cameras, which indeed has a tremendous impact in the detection distance of bright lamps at far distances.

Once bright objects are extracted, the segmented blobs are clustered, based on geometric characteristics of the blobs, in order to distinguish vehicles from other nuisance light sources. Each cluster is tracked in a sequence, using a Kalman Filter [13], obtaining a multi-frame tracking. Kalman filtering has been widely used in the literature for target tracking under the hypothesis of Gaussian distributions. Some examples of practical vision-based applications using Kalman filtering can be found in the literature such as for pedestrian detection [14,15] for multi-vehicle tracking.

We also perform a road vertical curvature estimation, due to the fact that at far distances the road may be not plane. Once, this road curvature is estimated, a vertical offset correction is only done for those objects located close to the horizon line, at the infinity. After that, some representative features are calculated for each tracked object, and then objects are classified in signs (main nuisance light source due to the reflections of the own vehicle's light over the road-traffic signs) or vehicles, using a support vector machine (SVM). Finally, a decision between the low/high beams turned on is taken.

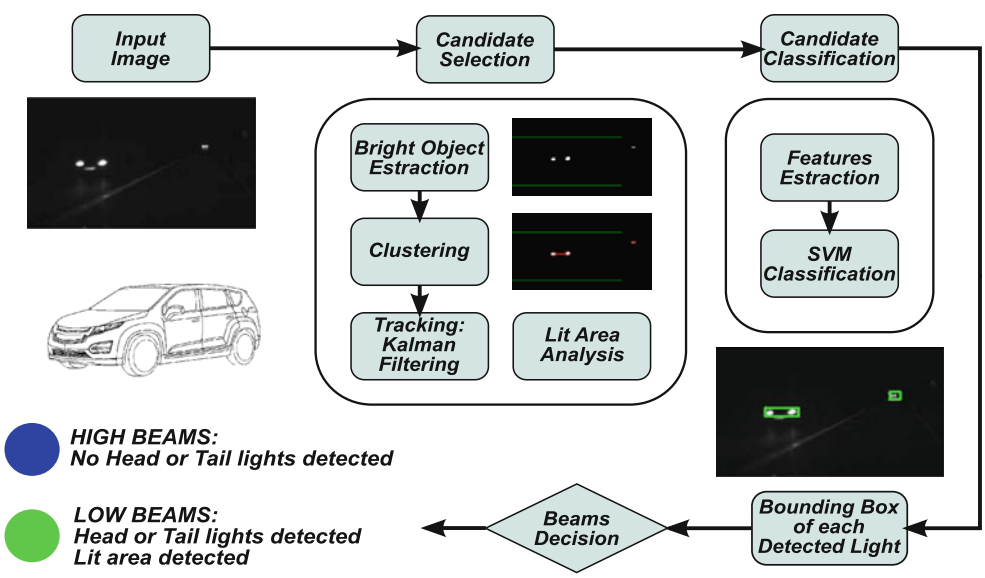

Fig. 4 Algorithm's overall overview for night-time images

Fig. 5 Typical night-time urban area environment

If the vehicle enters in an urban or well lit area, it is unnecessary to process all the algorithm steps. The bright objects segmentation is the only step which is processed, since in an urban or well lit area the amount of bright objects is higher than during night-time road conditions (Fig. 3) and traffic lamps usually appear in the first one-third of the vertical y-axis. According to this, when the number of bright objects is higher than a fixed threshold, the low beams output will be selected. This is because high beams are not necessary in urban areas where roads are well lit, since they are designed to help drivers see farther and drive safely within the area lit up by the high beams, in areas without much ambient light. Figure 5 depicts a typical night-time urban environment.

2.1 Bright objects segmentation

In our algorithm, B&W images are thresholded using an adaptive threshold in order to detect image bright objects and to measure some geometric parameters over them. Some important aspects must be considered for choosing a correct threshold value such as: road illumination conditions, vehicle's lights appearance, nuisance light sources and camera parameters.

Figure 6 depicts 3D intensity shape of a standard vehicle's head light. It has a Gaussian shape where the centre pixels belongs to the light source with values above 250. The edge pixels belong to the background with values below 50. As it can be seen, there is a high range in order to fix a threshold for light detection. Normally, nuisance light sources use to appear in the image with values below 200 (see Fig. 7b). The problem is that there are some reflections of road signs that present similar intensity values as the vehicle's light, as we depict in Fig. 7a. In these cases it is imposible to differentiate them using a thresholding method. Both images shown in Fig. 7 are from some of the analysed real sequences under our camera settings. Another related problem is that head and tail lights have different intensity values in the B&W image. Actually, intensity for tail lights is lower than for head lights and sometimes

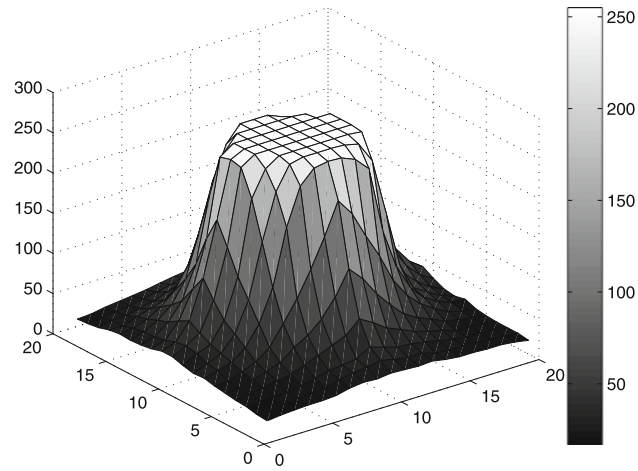

Fig. 6 Shape of vehicle's head light

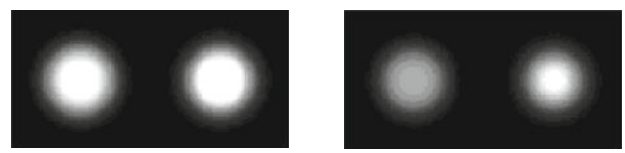

(a) Sign light vs Vehicle's head light

(b) Nuisance light vs Vehicle's tail light

Fig. 7 Grey scale difference between road sign, nuisance light, tail lights and head lights

below most of the nuisance artifacts in the image. This is the reason why tail lights detection is more difficult than head ones. Our adaptive thresholding technique is similar to the one described in [16]. The adaptive thresholding is computed as follows: firstly bright objects are extracted using a low threshold, and the mean and standard deviation (μ_i, σ_i) of the grey level of these objects are computed. These are weighted according to a Gaussian function of their distance from that centre point. We use a first very low threshold equals to 50 (in a grey level range from 0 to 255), to make sure that all the potential bright lights are extracted. Due to nuisance artifacts, a ratio aspect restriction is applied in the last step, in order to compute only the mean and standard deviation of potential vehicles lights. Later, bright objects are extracted from the original image according to this new adaptive threshold:

$$\text{Threshold} = \mu - k \cdot \sigma \tag{1}$$

$$\mu = \frac{1}{N} \cdot \sum_{i=1}^{N} \mu_i \tag{2}$$

$$\sigma = \frac{1}{N} \cdot \sum_{i=1}^{N} \sigma_i \tag{3}$$

In Eq. (1), the parameter k is set to a fixed value experimentally calculated in a setup process. With this thresh-

old, all bright objects are extracted correctly under different light conditions. Since the selected threshold depends on camera's gain and time exposure, the threshold can be tuned using this parameter k. As it will be explained in Sect. 2.5, we realized that in vehicle's lights a halo effect around lights appears, but this halo cannot be observed in the same magnitude in road signs, which means that could be a good parameter for classifying blobs between signs and vehicles. In order to measure this halo effect, we applied a black hat transformation [17]. This halo effect is more significant with saturated images, so as more saturation that we have in the image, it will be easier to classify and differentiate between bright lamps and nuisance artifacts or road signs reflections. According to this, our camera settings have a high exposure time and gain, which produce an acceptable blur and noise in the images for this application. Due to these high values, bright lamps appear in the images as saturated Gaussian shapes with some level of halo. With our thresholding algorithm, we are able to extract all the potential lights. Our algorithm is conservative in the way that we do not miss any real vehicular lamp in the segmentation, but we may introduce road sign reflections or nuisance artifacts in the next processing steps. However, introducing nuisance artifacts in this step of the algorithm is unavoidable and then we will classify correctly the segmented bright object by means of SVM as explained in Sect. 2.6.

Another approach for bright objects segmentation, is using the scale-normalized Laplacian operator. This operator is commonly used as a blob detector. Given an image $f(x, y)$, the image is convolved with a bi-dimensional gaussian kernel of standard deviation σ obtaining $L(x, y, \sigma)$. Equation (4) shows the scale-normalized Laplacian operator:

$$\nabla^2 L(x, y, \sigma) = \sigma^2 \cdot (L_{xx} + L_{yy}) \tag{4}$$

This operator has good responses for blobs of similar size to the scale parameter σ. The operator response is strongly dependent on the relationship between the size of the blob and the scale at which the Laplacian operator is computed. In order to automatically capture blobs of different size (unknown) in the image, a multi-scale approach is necessary [18]. In addition, the size in pixels of head lights and tail lights blobs in the image is approximately known under certain camera settings. Therefore, we apply the scale-normalized Laplacian operator at two different scales, one bigger scale (σ_1) for head lights and a smaller one (σ_2) for tail lights. Blobs with higher response in both scales are selected as bright objects. Figure 8 depicts the results of applying the scale-normalized Laplacian operator using a scale for head lights over the image of Fig. 3.

According to our camera's configuration, head lights and tail lights do not appear normally above the one-third of the vertical y-axis. That is the reason why a region of interest

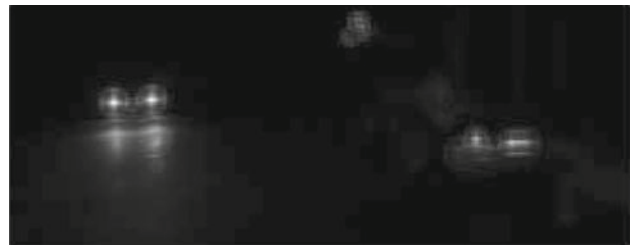

Fig. 8 Scale-normalized Laplacian operator for head lights

is used. Two lines (denoted as horizon lines) delimitate the interest area in the image. The *Horizon Real* is the value of the y image coordinate obtained by considering in the calibration equations that vehicles are located at the infinity ($Z \to \infty$). The *Horizon Low* is the value of the y image coordinate at where vehicles are considered to be at a distance Z of 5 m which is so close to the camera-assisted vehicle that no blob can appear below this line. Since in practice the road is not always planar, there can appear blobs over the real horizon and a new line called *Horizon Up* is defined. This is the real horizon with a negative offset just for defining the real analysis area.

Both approaches work well and are robust to lighting changes. Since we have real-time restrictions, the adaptive thresholding method was chosen, since the computational burden is lower than with the scale-normalized Laplacian operator. Figure 9b shows how bright objects are extracted from the original image. The green lines that appear in Fig. 9b define the region of interest of the image.

2.2 Clustering and matching process

The goal of this process is to cluster the detected blobs in the previous step. As long as a cluster in a frame is matched with the same cluster in the next frame, this is considered as an object, and must be evaluated to determine if the object is considered as a vehicle or not.

The clustering and matching process starts by finding the closest object of the previous frame to each blob in the current frame according to the Kalman filter prediction of the position of each of the objects. If the closest object exists, the blob is associated to that object. In the case that the closest object had already an associated blob, proximity between the two blobs is evaluated, and if it is suitable that both blobs belong to the same vehicle, the blob is added to the object's blobs list. This may happen with the two lights of a car as it approaches. A basic method for detecting if an object is formed by only one or more blobs is studying its horizontal and vertical projections. If any of these has more than one relative maximum that means that through this projection the object presents more than one blob. With this method, we can distinguish between lights and its reflections, or if the blob

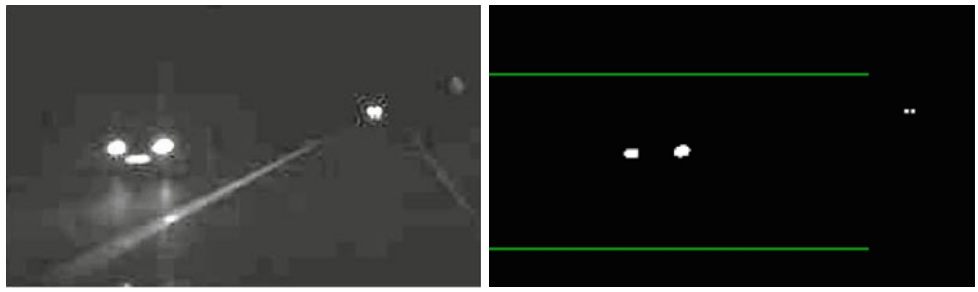

(a) Original image **(b)** Thresholded image

Fig. 9 Bright objects segmentation

is potentially a motorbike and/or a single lamp as is shown in Fig. 10.

Each object has a live time. This time counts the number of frames in which it has been matched. Objects must be matched during a minimum number of frames in order to be considered as valid. An important issue of the clustering process is to classify objects between preceding or oncoming vehicles. If ever an object is detected to be at a distance twice farther than any other distance at what it has been before, the object is classified as *preceding*, which means that the object is moving in the same direction of the camera-assisted car. For the rest of cases the object is classified as *oncoming*, which means that the object is moving in the opposite direction.

Then, objects are tracked using Kalman filters [13]. The state vector is simply the respective horizontal and vertical image coordinates for the centroid of every object. The purpose of this Kalman filtering is to obtain a more stable position of the object's centroid since from this position, we obtain the distance between objects and the camera-assisted car. In addition, car oscillations due to the unevenness of the road makes the screen coordinate of the detected lights change several pixels up or down. This effect makes the distance detection worse, so Kalman filtering is a good method for diminishing these kinds of oscillations. Another advantage of using Kalman filters is that we can predict during some frames the position of every object in situations where detection fails due to

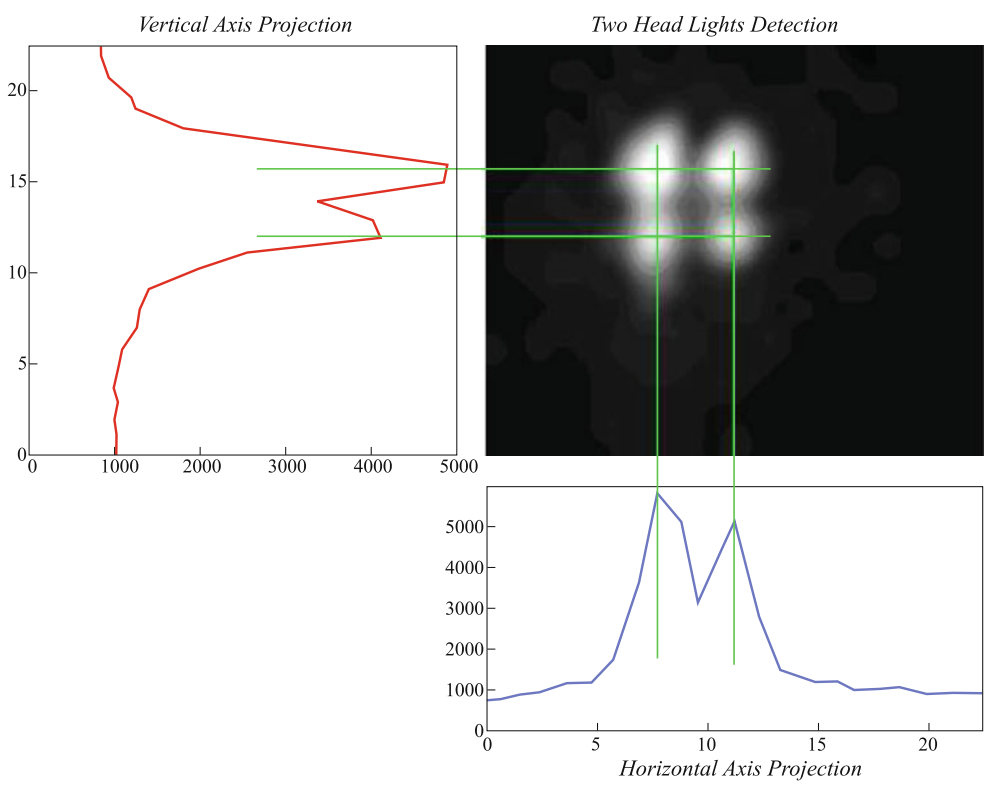

Fig. 10 Vertical and horizontal projections

occlussions, overtakings or distortion changes of the light sources.

2.3 Distance estimation

In order to estimate the distance between the camera-assisted car and the detected vehicles using monocular vision, a perspective camera model is applied, as it can be seen in Fig. 11. We take the seminal work of Dickmanns and Mysliwetz [19] as our main reference for camera look-ahead distance and road curvature estimations. By using the road vertical curvature estimation, we perform a correction of the vertical image coordinate of all the objects located at the infinity where the flat road assumption is not valid. The origin of the vehicle coordinate system is located at the central point of the camera lens. The X_V and Y_V coordinates of the vehicle coordinate system are parallel to the image plane and the Z_V axis is perpendicular to the plane formed by the X_V and Y_V axes. A vehicle at a look-ahead distance Z from the camera will be projected into the image plane at a vertical and horizontal coordinates (u, v), respectively. Vertical and horizontal mapping models can be carried out but in this application the most important is the vertical one. The vertical model considers that the road is flat and it uses the following parameters:

- I: Image
- Z: look-ahead distance for planar ground (m)
- h_{CAM}: elevation of the camera above the ground (m)
- LH_Y: elevation of the vehicle's light above the ground (m)
- θ_{CAM}: camera pitch angle relative to vehicle pitch axis (rad)
- θ_Z: incident angle of the precedent vehicle's light in the camera relative to vehicle pitch axis (rad)
- v: vertical image coordinate (pixels)
- *Height*: vertical size of the CCD (pixels)
- F_v: vertical focal length (pixels)

According to Fig. 11, the vertical mapping geometry is mainly determined by the camera elevation h_{CAM} and vehicle's lights elevation LH_Y above the local ground plane as well as the pitch angle (θ_{CAM}). The longitudinal axis of the vehicle is assumed to be always tangential to the road at the vehicle centre of gravity (cg).

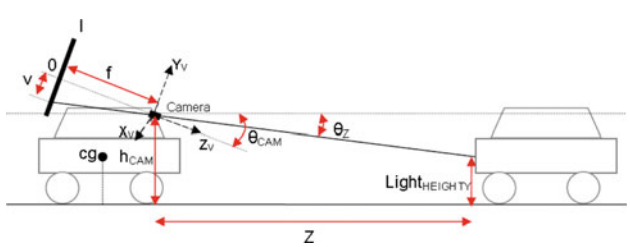

Fig. 11 Vertical road and mapping geometry

To each image scan line at v, there corresponds a pitch angle relative to the local tangential plane of:

$$\theta_Z = \theta_{\mathrm{CAM}} + \arctan\left(\frac{v}{F_v}\right) \tag{5}$$

From this, the planar look-ahead distance corresponding to v, is obtained as:

$$Z = \frac{h_{\mathrm{CAM}} - LH_Y}{\tan(\theta_Z)} \tag{6}$$

And finally, after applying a coordinate change in the image plane, the equation for computing the look-ahead distance Z becomes:

$$Z = \frac{h_{\mathrm{CAM}} - LH_Y}{\tan\left(\theta_{\mathrm{CAM}} + \arctan\left(\frac{v-\mathrm{Height}}{F_v}\right)\right)} \tag{7}$$

Even though this look-ahead distance estimation is reasonably good in almost all the scenarios, there are situations as uneven roads or when the detected vehicle is on a curve, where the horizontal mapping geometry must be considered, as we depict in Fig. 12. For this purpose a correction of the distance Z is proposed in which the projection in the horizontal coordinate of the image (u) is introduced:

$$Z_{\mathrm{AUX}} = \frac{Z \cdot (u - \mathrm{Width})}{F_u} \tag{8}$$

where u is the horizontal image coordinate (pixels), *Width* the horizontal size of the CCD (pixels), F_u is the horizontal focal length (pixels).

And finally the real distance (Z_{R}) can be obtained from the contributions of horizontal and look-ahead distances applying the following equation:

$$Z_{\mathrm{R}} = \sqrt{Z_{\mathrm{AUX}}^2 + Z^2} \tag{9}$$

The parameter LH_Y is defined as the elevation of the vehicle's light (head lights or tail lights) above the road. Since we are working with only one camera at night and estimating 3D distances very far, it is not possible to calculate this from the image analysis. Then, this parameter is computed off-line in a previous setup. As there are high differences between the elevation of the head and tail lights in vehicles, two different values were assigned to this parameter as a function of the kind of light. These values represent the average elevation of analysed vehicles in the setup process.

In addition, a classification between preceding or oncoming vehicles is carried out in the clustering stage of the algorithm based in aspect ratio constraints. Depending on this classification, one of the next two different values will be used:

- Head lights: $LH_Y = 0.6\,\mathrm{m}$

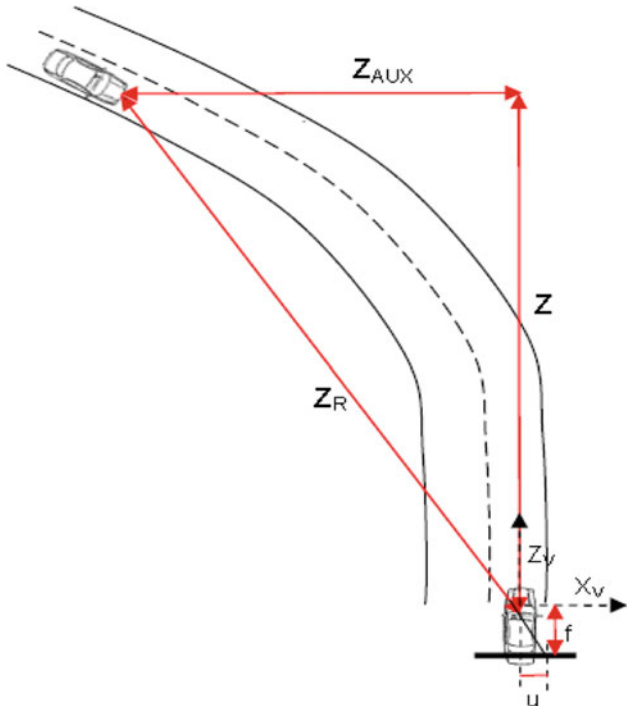

Fig. 12 Horizontal road and mapping geometry correction

- Tail lights: $LH_Y = 0.8\,\text{m}$

However, this distance is only an approximation, since some sources of error can affect this estimated distance, such as: elevation of the vehicle's light, road unevenness, object's centroid, etc. In order to minimize this errors, a vertical coordinate correction is proposed.

2.4 Road vertical curvature estimation and vertical coordinate correction

In our camera perspective model shown in Fig. 11, we are assuming that the road is plane. However, this is a dangerous assumption, since at far distances (for distances higher than 500 m) the road vertical curvature may influence the vertical position at which the objects appear in the image. As a symplifying assumption, the horizontal road curvature is assumed to be so small that is not considered in the perspective model. Figure 13 depicts the vertical road curvature problem. One of the most important parameters to classify between road signs reflections and vehicle's lights is the vertical image coordinate v. If the road vertical curvature is significant, some mistakes can arise in the classification process due to the flat road assumption, so a road vertical curvature estimation must be included into our camera perspective model. From the vertical geometry mapping we can obtain an expression for this vertical curvature:

$$C_{0v} = \frac{2}{Z_{\text{inf}}}\left[\tan\theta_Z - \frac{(h_{\text{CAM}} - LH_Y)}{Z_{\text{inf}}}\right] \tag{10}$$

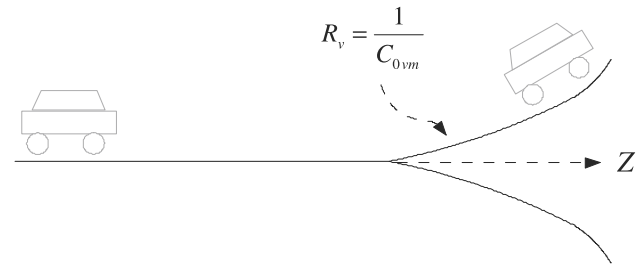

Fig. 13 Road vertical curvature problem

In the last equation, Z_{inf} is the distance Z at which we can consider that the object is located at the infinity. This parameter is set to a default value of 900 m. The parameter C_{0v} is computed for every object located close to the horizon line in the image and with a small size. Then, the parameter C_{0vm} is estimated as the mean of all the individuals C_{0v} and is introduced into a Kalman filter process to obtain a more stable estimation of the curvature. Then, the look-ahead distance with vertical curvature distance considering the non-planar road case is computed using the estimated road vertical curvature according to the method described in [19]. Finally, the look-ahead distance with vertical curvature Z_{cv} has the following expression:

$$Z_{cv} = \frac{\tan\theta_Z}{-C_{0vm}}\left[1 - \sqrt{1 + 2\cdot C_{0vm}\frac{(h_{\text{CAM}} - LH_Y)}{\tan^2\theta_Z}}\right] \tag{11}$$

From this new distance Z_{cv}, we can correct the vertical image coordinate v according to Eq. (12):

$$v = F_v \cdot \tan\left(\arctan\left(\frac{h_{\text{CAM}} - LH_Y}{Z_{cv}}\right) - \theta_{\text{CAM}}\right) + \text{Height} \tag{12}$$

2.5 Black hat transformation

It can be experimentally observed, that one indicative feature of headlights and taillights is the halo effect of the lights. This halo effect is no present in passive lamps, such as road signs or nuisance artifacts. For standing out the halo of the lights, the black hat transformation is proposed. The top-hat transformation is a powerful operator which permits the detection of contrasted objects on non-uniform background [17]. This transformation has been successfully used in intelligent transportation systems such as road-traffic monitoring for vehicle shadow detection [20]. There are two different types of top-hat transformations: white hat and black hat. The white hat transformation is defined as the residue between the original image and its opening. The black hat transformation is defined as the residue between the closing and the original image. The operations white and black hat transformations are defined as follows, respectively:

$$WH_T(x, y) = (f - f \circ B) \tag{13}$$

$$BH_T(x, y) = (f \bullet B - f) \tag{14}$$

In (13) and (14) $f(x, y)$ is a grey scale image and B is the structuring element. Both operators, white and black hat can be used in order to modify the contrast of the image or enhancing contrast in some regions of the image. Normally, in grey scale images, the local contrast is ruled by two kinds of features: bright and dark features. The white hat image contains local peaks of the intensity and the black hat image contains local valleys of the intensity. As we can stand out the effect of the halo (local valleys of intensity) of head lights or tail lights, the black hat transformation was chosen for this purpose. In fact, the halo is one of the most important parameters to distinguish between road signs and vehicles. This effect is more important for head lights since the intensity of these lights is higher than for tail lights. However, this effect is not signicant at distances farther than 200 m, since at these distances, head lights and tail lights usually appear in the image like a single lamp without halo. Figure 14 depicts the halo effect for a vehicle, and as can be seen in Fig. 15, this effect is not enough significant for road signs.

Once the transformation is done, an indicative parameter of the lights' halo called *hat* is computed as the average intensity of a defined rectangle including the object.

2.6 Classification using support vector machines

As it has been exposed in previous sections, one of the most important problems of the system is to distinguish between vehicle's lights and reflections of traffic signs (main nuisance light source). In this step, the detected bright objects are classified as signs or vehicles depending on some discriminant parameters using SVMs [11]. Two aspects are essential in the deployment of SVMs classifiers: the training strategy and the classifier structure. As SVMs are supervised learning methods used for classification, it is necessary to obtain

(a) Original image **(b)** Black hat image

Fig. 14 Halo effect for vehicles

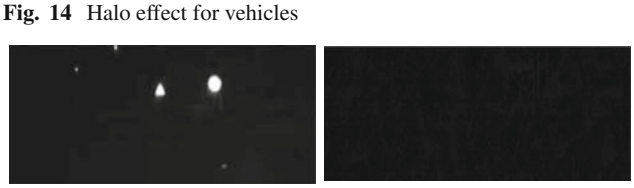

(a) Original image **(b)** Black hat image

Fig. 15 Halo effect for road signs

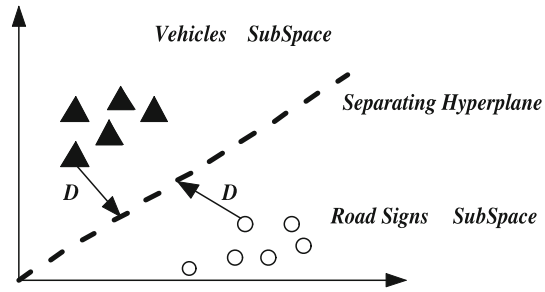

Fig. 16 Classification problem with SVMs

a model under supervised training (*training mode*), and once the model is obtained, it can be used in real applications (*test mode*). Figure 16 depicts an example of the SVMs classification problem, in which we have two different categories and we need to find the separating hyperplane between them.

Support vector machines map input vectors to a higher dimensional space where a maximal separating hyperplane is constructed. Two parallel hyperplanes are constructed on each side of the hyperplane that separates the data. The separating hyperplane is the hyperplane that maximizes the distance between the two parallel hyperplanes. An assumption is made that the larger the margin or distance between these parallel hyperplanes the better the generalization error of the classifier will be.

An input vector was defined for the classifier. This vector is composed of different parameters which are computed per object and define the state vector for the SVM. We use a set of features of different types mainly based in (1) binary (area, aspect ratio, etc.) and (2) intensity features (moments, mean intensity, standard deviation, etc.). In [7] they use similar binary and intensity features for their Adaboost learning to classify candidate objects as vehicles or non-vehicles. In addition, they also add colour information and features that measure the ratios between monochrome and red pixels. We can choose between a huge amount of binary and intensity features for classification. Experimentally, we have obtained the best results with the following set of features:

- Area in pixels
- Coordinate v of the object's centroid
- Hat Value
- Rectangularity
- Aspect ratio
- Length of the object's contour
- Circularity

The SVM model was also trained considering the Hu Moments invariants [21]. These moments are used in pattern recognition to provide a scale, orientation and position invariant characterization of a given object's shape. Hu's moments are based on normalized central moment, which are invariant to both translation and scaling. We used Hupkens and

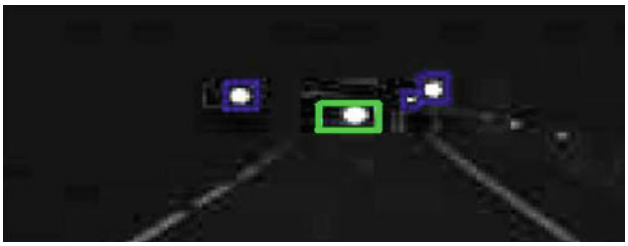

Fig. 17 Classification of objects at far distances

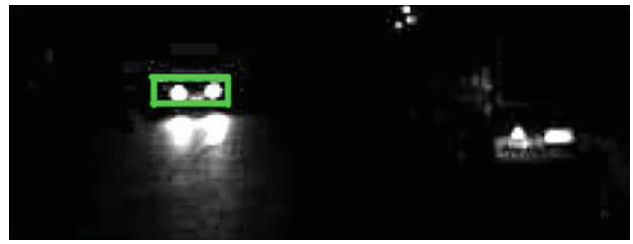

Fig. 18 Detection of an oncoming vehicle

de Clippeleir normalization [22] to increase the signal noise ratio.

The output of the SVM d, is simply the signed distance of the test instance from the separating hyperplane. This output indicates wether the analysed object corresponds to a vehicle or not, and can be used as a threshold for separating nuisance light sources and vehicles.

The classification algorithm uses this result and classifies the objects as signs or vehicles depending on its output distance from the separating hyperplane. The classification between vehicles and nuisance lights is more difficult at far distances. This problem can be seen in Fig. 17 where one vehicle located close to the horizon line in the image (at a distance of approximately 200 m) is surrounded by several signs and the system classified each of the objects correctly (headlights in green and road signs in blue).

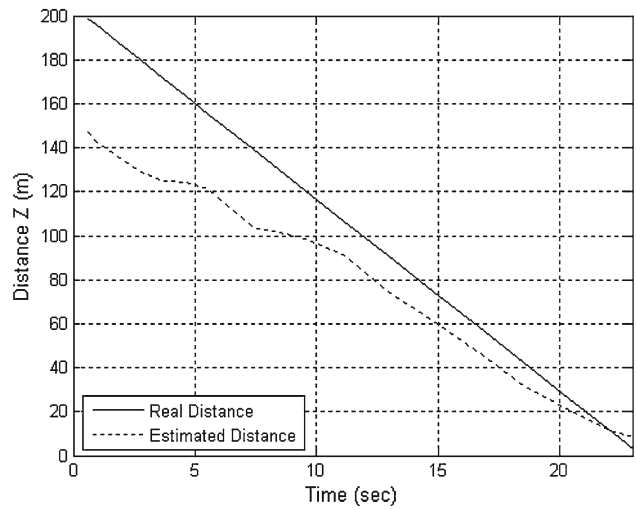

Fig. 19 Distance estimation 200–0 m. Head lights

3 Experimental results

The system was implemented on a Pentium IV 3 GHz platform and the size of the recorded image sequences is 752 pixels × 480 pixels per frame so as to detect vehicles at far distances. The computation time spent on processing one input frame depends on the complexity of the road scene (mainly on the number of blobs and objects to be processed). The frame rate of the system is in average close to 20 frames/s which is enough for real-time demands. Experimental tests (more than 7 h of video sequences) under different night-time road scenes and different weather conditions (dry, rainy, foggy, freezing) were done for analyzing the performance of the system. The B&W micro-camera and the rest of hardware requirements were mounted in a C4-Picasso Ficosa's prototype car. The experimental tests were carried in different roads of Mollet del Vallés (Barcelona, Spain) and Vigo (Pontevedra, Spain), including some sequences under rainy conditions.

3.1 Distance estimation

3.1.1 Head lights

One sequence was tested in which a vehicle was placed at a distance of 200 m in front of the camera-assisted car. Then, the vehicle approached from a distance of 200 m to a distance of 0 m with a constant speed of 30 km/h. The purpose of the sequence was to detect and track the vehicle's head lights so as to evaluate the accuracy of the distance estimation. Figure 18 depicts a sample of the scenario for the distance estimation analysis. The results of this analysis can be seen in Fig. 19.

3.1.2 Tail lights

For the tail lights case, other sequence was tested in which a vehicle was placed at the same distance than the camera-assisted car and then the vehicle advances from a distance of 0 m to a distance of 200 m with a constant speed of approximately 25 km/h. Figure 20 depicts a sample of the scenario for this distance estimation analysis. The results of this analysis can be seen in Fig. 21.

According to the results, it can be observed that the estimated distance is a little worse for the tail lights case, due to the fact that the luminance of tail lights is lower than the luminance of head lights, and also the size of tail lights is smaller than the size of head lights. In addition, the distance estimation error is higher for vehicles located at far distances.

Fig. 20 Detection of a preceding vehicle

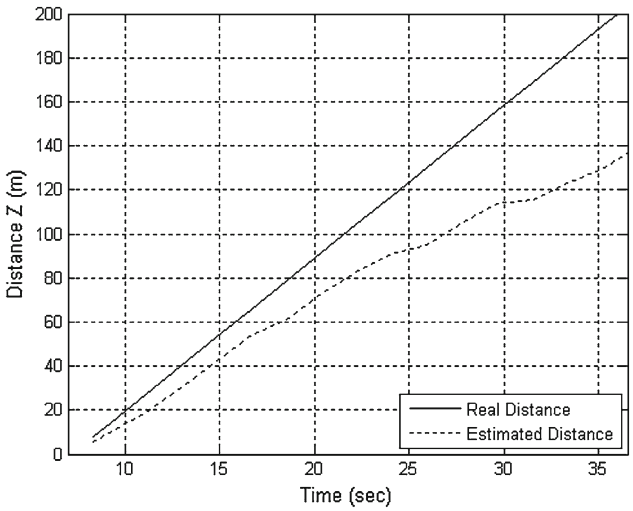

Fig. 21 Distance estimation 0–200 m. Tail lights

Table 1 Total number of instances training mode

Objects type	Total number of instances
Vehicles	46,835
Signs	22,345

Table 2 Total number of instances test mode

Objects type	Total number of instances
Vehicles	1,182
Signs	1,110

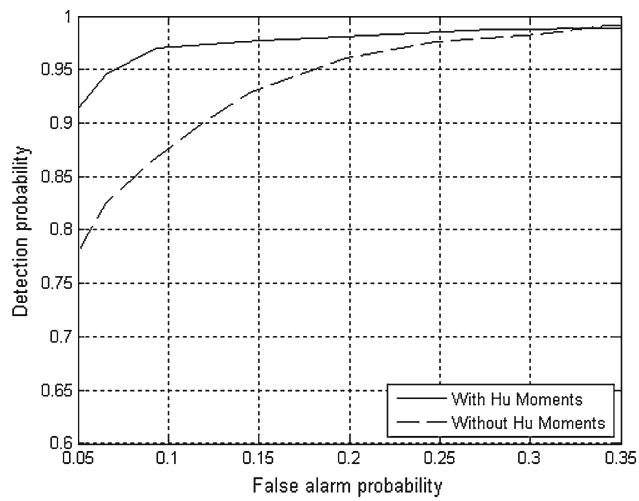

Fig. 22 Receiver operating characteristic

Table 3 Test sequences: obtained probabilities

Probability	Without Hu moments	With Hu moments
P_D	0.8646	0.9458
P_{FA}	0.0914	0.0659

3.2 Analysis of the classifier

The SVM was trained using a representative database for learning and testing. For creating the training and test sets, the ratio between positive (vehicles) and negative (mainly reflections of traffic signs) must be set to an appropriate value in order not to produce misslearning or a high percentage of false positive detections (signs classified as vehicles) during on-line tests [11]. The number of training and test sets is shown in Tables 1 and 2, respectively.

The quality of the classifier is measured by the probability of detection P_D (objects that are classified correctly) and the probability of false alarm P_{FA} (vehicles that are classified as signs and vice versa). These two indicators are shown together in Fig. 22. This figure depicts also a comparison of the classifier's performance using Hu's invariant moments and without these moments.

As it can be observed, the performance is better incorporating Hu's invariant moments to the classifier. For the test sequences, the obtained false alarm and detection probabilities are shown in Table 3.

3.3 Head lights detection

In this section performance of head lights detection is provided. For this purpose, some video sequences were processed and some important parameters were computed in order to evaluate the performance of the system.

In Table 4, results about head lights detection are shown. It is not reliable to show results about distance detection, since the system is thought to detect head lights at far distances (more than 200 m), and at these distances, the estimation error is high as it has been shown in Sect. 3.1. Instead, a most interesting and reliable parameter as is *Time Delay* will be calculated. This parameter gives the delay in time between the first moment when a vehicle is seen by the camera and the moment when the vehicle is detected correctly by the algo-

Table 4 Head lights detection results

No. of sequence	Total time (min:s)	Head lights count	Detection rate %	Time delay (s)	Time delay R_{VC} (s)
1	1:02	6	100	1.73	0.5
2	1:02	4	100	3.8	0.82
3	1:01	6	100	0.51	0.17
4	0:52	4	100	3.72	1.12
5	0:55	2	100	0.23	0.17
6	1:03	8	100	0.25	0.17
7	1:07	2	100	1.18	0.17
8	0:58	10	100	0.3	0.17
9	1:09	26	100	0.46	0.17
10	1:03	4	100	0.93	0.17

rithm. It also includes the mimimum number of frames for the object to be considered as valid. The minimum number of frames for an object to be considered as valid, was heuristically set to five frames, which in time is equivalent to 0.17 s considering 30 frames/s. A comparison without considering the road vertical curvature and considering it was done. This comparison shows how the road vertical curvature estimation reduces this delay for objects located at far distances. In Table 4 the *Time Delay* field is the mean time delay of all the head lights in the analysed sequence. The field *Time Delay* R_{VC} denotes the mean time delay considering the road vertical curvature estimation.

The main conclusion is that all the head lights are detected, but the problem is when these head lights are detected. The detection rate is always 100%, since no matter how far a light is, the system is going to detect and classify correctly the lights sooner or later, the main problem is when this light is detected and correctly classified. Some head lights may be detected too late and this is due to the road unevenness at far distances. This type of problem is shown in Fig. 23. In this figure one oncoming vehicle is located at a distance of approximately 600 m. Due to road unevenness at these far distances, the vertical image coordinate v is above the horizon line. In fact, the value for this coordinate in the sample is a typical value for road signs. Since the coordinate v is one of the most important parameters in the classification process, due to its value, the SVM classifies the object as a road sign, which is wrong. Then, after 88 frames (3.52 s) the object is classified correctly as a vehicle. A delay of about 3 s in switching between high beams to low beams may be very dangerous depending on road-traffic conditions. With the estimation of the road vertical curvature, the coordinate v is corrected and the vehicle is detected and classified correctly immediately.

The system can detect head lights for first time at distances between 300 and 500 m, depending on road conditions. In some experimental tests that were done in planar roads some

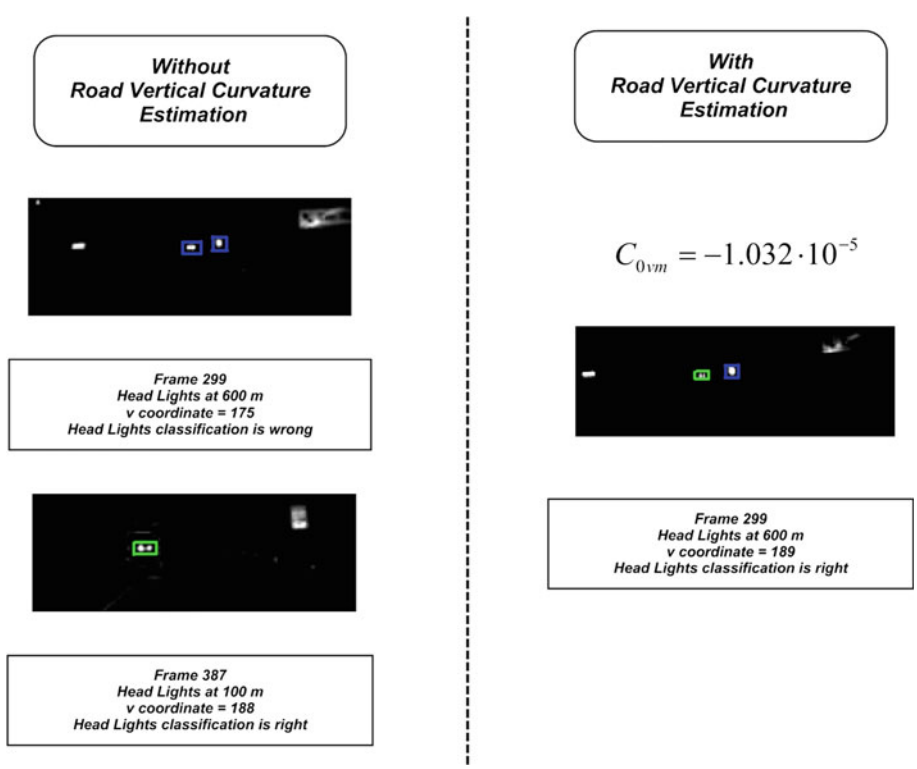

Fig. 23 Problematic of using flat road assumption

vehicles where detected even at 700 m, which is a very good performance, since it is really difficult to detect and classify objects correctly at these distances.

3.4 Tail lights detection

In Table 5 the results of the tail lights detection are shown. In this case, the road vertical curvature estimation is not as important as in the head lights case, where distances farther than 200 m are considered. The reason for this, is that for distances close to 200 m or farther, the size of tail lights in pixels is so small that it is impossible to classify and detect them correctly.

Tail lights are more difficult to be detected than head lights using a B&W camera. This is because the luminance of the tail lights is lower than luminance of the head lights, and also the size of the tail lights is smaller than the size of the head lights. Tail lights are basically characterized by its red colour and they can be detected in an easier way with a red filter. Besides, the variety and diversity of tail lights is very large which makes the detection more difficult. This means that detection of tail lights depends so much on the vehicle type.

The large time delay in sequence 14 is due to this problem. In this sequence, a truck appears in the same lane of the camera-assisted vehicle at a distance about 70 m. Trucks tail lights usually consist of two pairs of lights, one pair at the bottom and the other pair at the top of the truck's rear part. The truck's tail lights are very weak so the system cannot detect correctly its tail lights until the truck is at a distance of about 30 m, and even at 30 m the size of the tail lights in the image is about 3–5 pixels which is a very small amount of pixels for processing the object correctly. Figure 24 depicts an image of truck's tail lights at a distance of 30 m.

3.5 Comparison with state of the art methods

Even there are few references in specialized scientific journals and symposiums, we want to show a comparison of our method against the others, and show the benefits and problems of our proposal. Table 6 shows this comparison taken into account the following parameters:

Table 5 Tail lights detection results

No. of sequence	Length (min:s)	Tail lights count	Detection rate %	Time delay (s)
11	1:04	2	100	0.17
12	0:58	4	100	0.3
13	1:02	2	100	4.4
14	0:59	2	100	15.7

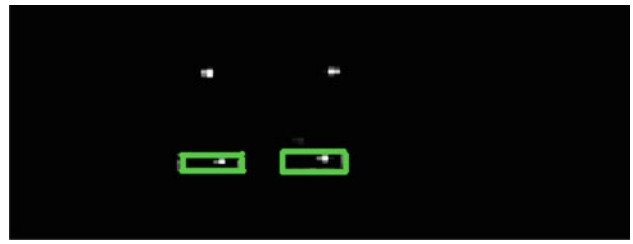

Fig. 24 Sequence 14 truck's tail lights at 30 m

- *Sensor type*: if the sensor used for the camera is B&W, RGB or contains both monochrome and colour sensors. The decision about the camera sensor has an important factor in the distance of detection for head and tail lights.
- *Detected lamps*: if the algorithm is able to detect head and tail lights or only one of them.
- *Classification method*: for methods that detect head and tail lights, the classification of objects between vehicular lamps and reflections or nuisance artifacts is extremely important. In this field, we show information about the Machine Learning and Pattern Recognition scheme that has been used for each of the algorithms.
- *Head and tail lights distance of detection* (m): we show information about the distance of detection at which head lights and/or tail lights are detected and classified correctly as vehicular lamps. We show approximated distances of detection, since all of the analysed works just give a qualitative analysis, impressions or just some distance estimates on some single frames.

The most similar work in the literature to ours is López et al. [7]. They divide the classification problem between small and non-small blobs, and have obtained very good classifier performances for head lights and tail lights, over 90% for non-small blobs and a worse for small tail lights 60%. Our classification mistakes between vehicles and road signs, are very low ($P_D = 0.9458$, $P_{FA} = 0.0659$) better than the ones obtained by López et al. However, as we are using a B&W, we only have one classifier between vehicles and road signs reflections, not distinguishing in the classification procedure between small, non-small blobs, head lights and tail lights. In addition, in the work by López et al. they do not perform any road curvature analysis estimation. The centroid of each bright object is one of the most important features in their AdaBoost learning scheme and since most of traffic lamps usually appear in the first one-third of the vertical y-axis, the road vertical curvature may influence the vertical position at which the objects appear in the image. We think that performing an analysis of the road vertical curvature and correcting the position of the centroid can increase classifier ratios, since according to our experiments the vertical position of each blob is very important in the classification

Table 6 Comparison of state of the art methods: sensor type, detected lamps, classification method and distance of detection for head lights and tail lights

References	Sensor type	Detected lamps	Classification method	Head lights distance (m)	Tail lights distance (m)
Chen [5]	RGB	Head lights Tail lights	Rule-based vehicle indentification	30	10
O'Malley et al. [6]	RGB	Tail lights	Aspect ratio constraints	–	30
López et al. [7]	75% Monochrome 25% Red	Head lights Tail lights	AdaBoost	300	300
LightBeam Controller	B&W	Head lights Tail lights	SVM	500	200

procedure. Furthermore, according to the results shown in the work by Enzweiler and Gavrila [23], we hypothesize that classification results using SVMs are better than with AdaBoost, at the cost of increasing the computation time, since one of the advantages of AdaBoost over SVMs is that they provide high performance and the computation time is small than with SVMs. However, if the dimension of the feature vector is small, we can still use SVM in real-time applications as it is our case. The works of Chen [5] and O'Malley et al. [6] do not address the problem of classification, just consider aspect ratio constraints to pair all the potential lights into a same vehicle. The main drawback of these works is that their distance detections ratios are very low for intelligent headlight controllers.

4 Conclusions and future work

In this paper, we have presented a night-time detection computer system for driving assistance. On the one hand, the system performance is satisfactory for head lights (detection range up to 300–500 m) but on the other hand, the performance for tail lights (detection range up to 50–80 m) must be improved. One advantage of the system is that works in real-time conditions. The computation time spent on processing one input frame depends on its road scene complexity and the number of blobs. In average the processing frame rate is close to 20 fps, which satisfies real-time demands. The classification mistakes between vehicles and road signs, are very low ($P_D = 0.9458$, $P_{FA} = 0.0659$), and can be improved considering more distinctive invariant features and increasing the size of the training and test data.

The results are encouraging, and we plan to include several improvements to the current implementation. More work must be done in the classification process in order to increase the accuracy of the classifier. Special attention is devoted in the classifier trying to incorporate new invariant parameters such as the Gaussian curvature or one and second order derivatives. In addition, multi-scale top-hat transformations can help in the halo detection at far distances. In order to achieve a more reliable distance estimation, some parameters such as the blob size, distance between blobs and the relative growth/shrinking in the the image can be fused to obtain a better estimation. As a future idea, a red filter is going to be introduced into the system in order to increase tail lights detection range up to 400 m.

Acknowledgments This work has been funded by the multinational company FICOSA INTERNATIONAL and was done in collaboration with Automotive Technological Center of Galicia (CTAG) as part of the DEMOCAR 1 project. The work was supported in part by the Spanish Ministry of Science and Innovation (MICINN) under Grant TRA2008-03600/AUT (DRIVER-ALERT Project).

References

1. U.S. Department of Transportation: Regulations of the light emissions of vehicle high beam headlamps (2007). http://www.dot.gov/
2. Akashi, Y., Rea, M.: The effect of oncoming headlight glare on peripheral detection under a mesopic light level. In: Progress in Automotive Lighting (2001)
3. GENTEX: Vehicle lamp control (2005). http://www.patentstorm.us/patents/6947577-fulltext.html
4. Mobileye: Adaptative headlight control (2007). http://www.mobileye-vision.com/
5. Chen, Y.L.: Nighttime vehicle light detection on a moving vehicle using image segmentation and analysis techniques. WSEAS Trans. Comput. **8**(3), 506–515 (2009)
6. O'Malley, R., Glavin, M., Jones, E.: Vehicle detection at night based on tail-light detection. In: 1st International Symposium on Vehicular Computing Systems, Trinity College Dublin (2008)
7. López, A., Hilgenstock, J., Busse, A., Baldrich, R., Lumbreras, F., Serrat, J.: Nighttime vehicle detection for intelligent headlight control. In: ACIVS 08: Proceedings of the 10th International Conference on Advanced Concepts for Intelligent Vision Systems, pp. 113–124. Springer, Berlin (2008)
8. Freund, Y., Schapire, R.E.: A decision-theoretic generalization of on-line learning and an application to boosting. In: Proceedings of the European Conference on Computational Learning Theory, pp. 23–37 (1995)
9. Alcantarilla, P.F., Bergasa, L.M., Jiménez, P., Sotelo, M.A., Parra, I., Fernández, D., Mayoral, S.S. : Night time vehicle detection for driving assistance. In: IEEE Intelligent Vehicles Symposium (IV) (2008)
10. Clanton, J.M., Bevly, D.M., Hodel, A.S.: A low-cost solution for an integrated multisensor lane departure warning system. IEEE Trans. Intell. Transp. Syst. **10**, 47–59 (2009)
11. Parra, I., Fernández, D., Sotelo, M.A., Bergasa, L.M., Revenga, P., Nuevo, J., Ocaña, M., García, M.A.: A combination of fea-

ture extraction methods for SVM pedestrian detection. IEEE Trans. Intell. Transp. Syst. **8**(2), 292–307 (2007)
12. Otsu, N.: A threshold selection method from gray-level histograms. IEEE Trans. Syst. Man Cybern. **9**, 62–66 (1979)
13. Welch, G., Bishop, G.: An introduction to the Kalman filter. Tech. Rep., University of North Carolina at Chapel Hill, Department of Computer Science (2001)
14. Bertozzi, M., Broggi, A., Fascioli, A., Tibaldi, A.: Pedestrian localization and tracking system with Kalman filtering. In: IEEE Intelligent Vehicles Symposium (IV), pp. 584–589 (2004)
15. Dellaert, F., Thorpe, C.: Robust car tracking using Kalman filtering and Bayesian templates. In: Conference on Intelligent Transportation Systems (1997)
16. Jain, A.: Fundamentals of Digital Image Processing. Prentice-Hall, Englewood Cliffs (1986)
17. Derong, Y., Yuanyuan, Z., Dongguo, L.: Fast computation of multiscale morphological operations for local contrast enhancement. In: IEEE Medicine and Biology 27th Annual Conference (2005)
18. Lindeberg, T.: Feature detection with automatic scale selection. Int. J. Comput. Vis. **30**(2), 77–116 (1998)
19. Dickmanns, E.D., Mysliwetz, B.D.: Recursive 3-D road and relative ego-state recognition. IEEE Trans. Pattern Anal. Mach. Intell. **14**(2), 199–213 (1992)
20. Alcantarilla, P., Sotelo, M.A., Bergasa, L.M.: Automatic daytime road traffic control and monitoring system. In: IEEE Intelligent Transportations Systems Conference (ITSC), pp. 944–949 (2008)
21. Hu, M.: Visual pattern recognition by moments. IRE Trans. Inf. Theory **8**(2), 179–187 (1962)
22. Hupkens, T.M., de Clippeleir, J.: Noise and intensity invariant moments. Pattern Recognit. **16**, 371–376 (1995)
23. Enzweiler, M., Gavrila, D.M.: Monocular pedestrian detection: survey and experiments. IEEE. Trans. Pattern Anal. Mach. Intell. **31**(12), 2179–2195 (2009)

Author Biographies

P. F. Alcantarilla is a PhD candidate at the Department of Electronics of Universtiy of Alcalá (Madrid, Spain) and a member of the RobeSafe research group. He works in the areas of Computer Vision and Robotics under the supervision of Dr. Luis Miguel Bergasa. His work is focused on using computer vision techniques such as SfM (Structure from Motion) or SLAM (Simultaneous Localization and Mapping) for assisting visually impaired users during navigation by either providing them information about their current position and orientation, or guiding them to their destinations through diverse sensing modalities. Before starting his PhD in 2008, he obtained a MSc in Electrical and Electronic Engineering from the University of Alcalá in 2006. In 2007 he did master studies in Biomedical Engineering at Linköping University. During his PhD, he has done several research internships at Georgia Institute of Technology (2008), Imperial College London (2009) and AIST, Tsukuba (2010). Since 2009, he is one of the co-founders of Vision Safety Technologies Ltd, a spin-off company established to commercialize computer vision systems for road infrastructure inspection.

L. M. Bergasa received the M.S. degree in Electrical Engineering in 1995 from the Technical University of Madrid and the PhD degree in Electrical Engineering in 1999 from the University of Alcalá, Spain. He is currently an Associate Professor at the Department of Electronics of the University of Alcalá. He has been the Head of the Department of Electronics in the period 2004–2010. He is the Coordinator of the RobeSafe Research Group from 2010. His research interests include real-time computer vision and its applications, particularly in the field of robotics, assistance systems for elderly people and intelligent transportation systems. He is the author of more than 120 refereed papers in journals and international conferences, and corresponding author of 6 national patents and 1 PCT patent. He has been the recipient of the first prize in the III contest of ideas for the creation of technology-based companies at the University of Alcalá in 2008, the Best Research Award for the 3M Foundation Awards in the category of Industrial in 2004, the Best Spanish PhD Thesis Award in Robotics conceded by the Automatic Spanish Committee in 2005, as director of the work, and the second prize in the Eduardo Barreiros Foundation Award to the Best Research Work on the Automotive field in Spain in 2010, as director of the work. He is associate editor of the Physical Agents Journal and a habitual reviewer in 10 journals included in the JCR index. He has served on Program/Organizing Committees in more than 10 conferences. He is IEEE member of the Robotics and Automation Society Technical Committee on Autonomous Ground Vehicles and Intelligent Transportation Systems as well as a member of the Computer Science Society. In 2009 he co-founded the first spin-off company of the University of Alcalá established to commercialize computer vision systems for road infrastructure inspection.

P. Jiménez received the MS degree in Telecommunications Engineering from the University of Alcalá, Alcalá de Henares (Madrid) in 2005, and he is candidate for the PdD degree, expected March 2011. He started as a researcher at the University of Alcalá in 2004, and since them has tackled problems in Electronics, FPGAs and computer vision. In the last field, he has worked in automotive and face-tracking applications.

I. Parra received his MS degree in Telecommunications Engineering and PhD degree in Electrical Engineering from the Universidad de Alcalá (UAH), Alcalá de Henares, Spain, in 2005 and 2010, respectively. He is currently a member of the Research Staff with the Departamento de Automática, Escuela Politécnica Superior, UAH. His research interests include intelligent transportation systems, intelligent vehicles, artificial vision and operating systems. Dr. Parra was the recipient of the Master's Thesis Award in eSafety from the ADA Lectureship at the Technical University of Madrid, Madrid, Spain, in 2006 and the 3M Foundation Awards under the category of eSafety in 2009.

D. F. Llorca received his MSc and PhD degrees in Telecommunications Engineering from the University of Alcalá (UAH), Madrid in 2003 and 2008, respectively. He is currently working as an Associate Professor at UAH. His research interests are mainly focused on computer vision and intelligent transportation systems. Dr. Llorca was the recipient of the Best PhD Award by the UAH, the Best Research Award in the domain of Automotive and Vehicle Applications in Spain in 2008, the 3M Foundation Awards under the category of eSafety in 2009, the Master Thesis Award in eSafety from ADA Lectureship at the Technical University of Madrid in 2004 and the Best Telecommunication Engineering Student Award by IVECO in 2004.

M. A. Sotelo received the Dr. Ing. degree in Electrical Engineering from the Technical University of Madrid, Spain, in 1996 and the PhD degree in Electrical Engineering from the University of Alcalá, Madrid, in 2001, where he is currently a full professor. He has been serving as an auditor and expert for the FITSA Foundation, working on R&D projects on automotive applications since September 2004. He is the author of more than 160 refereed publications in international journals, book chapters, and conference proceedings. His research interests include real-time computer vision and control systems for autonomous and assisted intelligent road vehicles. Dr. Sotelo is a member of the IEEE Intelligent Transportation Systems (ITS) Society and the ITS-Spain Committee. He was the recipient of the Best Research Award in the domain of Automotive and Vehicle Applications in Spain in 2002 and 2009, the 3M Foundation Awards under the category of eSafety in 2003 and 2004, and the Best Young Researcher Award from the University of Alcalá in 2004. He is currently an Associate Editor of IEEE Transactions on Intelligent Transportation Systems.

S. S. Mayoral received her BSc in Mathematics and MSc in Computer Science from the Universitat Autònoma de Barcelona (UAB), Barcelona, Spain, in 1999 and 2000, respectively. In 2000, she joined the Computer Vision Center where she was involved in several industrial projects as R&D Machine Vision Engineer. From 2005 to 2009, she developed advanced driver assistance systems in Ficosa International. Currently, she holds the position of Senior Vision Engineer in ADASens. Her main research interests include machine Vision, object recognition, advanced driver assistance systems and performance evaluation.